# MOLTEN SALT REACTOR FUEL DEPLETION TOOLS IN SCALE[1]

Benjamin R. Betzler, Kursat B. Bekar, William A. Wieselquist, Shane W. Hart, and Shane G. Stimpson

*Oak Ridge National Laboratory, P.O. Box 2008, Oak Ridge, TN, betzlerbr@ornl.gov*

*Molten salt reactor depletion modeling and simulation tools have been implemented into the SCALE suite for reactor analysis and design developed by Oak Ridge National Laboratory. For depletion with material feeds and removals, additional removal and feed rate functionalities are being developed in ORIGEN to account for these flows during depletion. To track separate fuel and waste materials, additional functions and an iterative scheme are being added to the SCALE/TRITON lattice physics tool. The functionality of these tools has been demonstrated in part for previous analyses using external scripts that manage SCALE/TRITON calculations. Direct implementation of these functionalities into SCALE provides for a more efficient, more accurate material accountability methodology that is accessible to external SCALE users with a new input definition. These implementations are being tested for accuracy and to demonstrate their applicability to predefined molten salt reactor use case problems. This work demonstrates the capability of the SCALE modeling and simulation tools for reactor physics and fuel cycle analysis of molten salt reactor concepts.*

## I. INTRODUCTION

Oak Ridge National Laboratory (ORNL) has recently undertaken work to advance the technology readiness level of a software package capable of calculating molten salt reactor (MSR) fuel composition and reactivity changes during operation. This work will prepare a prototype MSR neutronics tool that can be further applied to specific MSR designs, including those being developed by several private companies (e.g., Terrestrial Energy, FLiBe Energy). The recent $1.3 billion private investment in advanced reactor technology detailed in a Third Way report [1] includes several of these leading liquid-fueled MSR concepts, indicating a growing need for an MSR neutronics and fuel cycle tool, along with additional MSR transient and heat transfer analysis tools.

While products from universities or internally developed tools provide partial capabilities for liquid fueled MSR analysis, there is currently no established tool for neutronics and for fuel cycle design and evaluation of liquid-fueled MSRs. Significant work in fast and thermal MSR analysis has yielded workable tools that aim to solve these issues [2, 3, 4, 5, 6, 7, 8]. Recent work at ORNL to develop software with these capabilities has established proven methods and concepts. Initial development of these methods used external Perl scripts to enable the analysis of a liquid-fueled system with a solid-fueled reactor analysis tool [9]. This method evolved into a generic Python script known as ChemTriton, which relies on the same methodology, but provides more flexibility to analyze realistic scenarios in MSR operations [10].

For neutronic and fuel cycle analysis, the two most important factors are (1) depletion with continuous removals and (2) delayed neutron precursor flow [11]. Any tool designed to properly model neutron transport and depletion in a fluid-fueled system must account for both of these phenomena. Implementation of these tools into SCALE [12] stands to benefit a larger number of analysis tools, as many tools use ORIGEN [13] for depletion calculations. This includes benefits to Shift [14] and other tools that use ORIGEN through its application program interface.

This article discusses the theoretical underpinnings of depletion with continuous removals, the numerical implementations of these developed models, testing of the implementations, and simulation of representative MSR use case scenarios.

## II. THEORY

SCALE implementation for these methods requires development in several tools within the code's base, including the point depletion solver ORIGEN and the neutron transport-depletion coupling interface in SCALE/TRITON.

ORIGEN solves the system of ordinary differential equations (ODEs) that describe nuclide generation, depletion, and decay [12],

$$\frac{dN_i}{dt} = \sum_{j\neq i}\left(l_{ij}\lambda_j + f_{ij}\sigma_j\phi\right)N_j(t) - \left(\lambda_i + \lambda_{i,\mathrm{rem}} + \sigma_i\phi\right)N_i(t) + S_i(t), \quad (1)$$

where
$N_i$ is the amount of nuclide $i$ (atoms),
$\lambda_i$ is the decay constant of nuclide $i$ ($s^{-1}$),
$\lambda_{i,\mathrm{rem}}$ is the removal constant defining the continuous removal of nuclide $i$ ($s^{-1}$),
$l_{ij}$ is the fractional yield of nuclide $i$ from decay of nuclide $j$,
$\sigma_i$ is the spectrum-averaged removal cross section for nuclide $i$ (barn),
$f_{ij}$ is the fractional yield of nuclide $i$ from neutron-induced removal of nuclide $j$,
$\phi$ is the angle- and energy-integrated, time-dependent neutron flux (neutrons/$cm^2$-s), and

$S_i$ is the time-dependent source/feed term (atoms/s).

This may be written in matrix form as

$$\frac{d\boldsymbol{N}}{dt} = \mathbf{A}\boldsymbol{N}(t) + \boldsymbol{S}(t), \tag{2}$$

where $\mathbf{A}$ is a size-$M$ (number of nuclides considered) square matrix known as the transition matrix, and the nuclide concentration and source terms are column vectors. Rewriting this equation as its transpose yields

$$\frac{d\boldsymbol{N}^{\mathrm{T}}}{dt} = \boldsymbol{N}^{\mathrm{T}}(t)\mathbf{A}^{\mathrm{T}} + \boldsymbol{S}^{\mathrm{T}}(t), \tag{3}$$

which describes the same system of equations, with the nuclide concentration and source terms as row vectors. The transpose of the transition matrix has the structure

$$\mathbf{A}^{\mathrm{T}} = \begin{bmatrix} -\lambda_1 - \lambda_{1,\mathrm{rem}} - \sigma_1\phi & \cdots & l_{M1}\lambda_1 + f_{M1}\sigma_1\phi \\ l_{12}\lambda_2 + f_{12}\sigma_2\phi & \cdots & l_{M2}\lambda_2 + f_{M2}\sigma_2\phi \\ \vdots & & \vdots \\ l_{1M}\lambda_M + f_{1M}\sigma_M\phi & \cdots & -\lambda_M - \lambda_{M,\mathrm{rem}} - \sigma_M\phi \end{bmatrix}, \tag{4}$$

and is considerably sparse, with approximately 1% of the matrix elements as non-zero. In this formulation, $\mathbf{A}^{\mathrm{T}}$ may be interpreted as an incomplete description of a continuous-parameter Markov chain, where the parameter space is continuous time and the countable state space consists of nuclides. Continuous-parameter Markov chains are characterized by the transition intensity, or transition rate, matrix

$$\mathbf{Q} = \begin{bmatrix} -q_1 & q_{12} & \cdots \\ q_{21} & -q_2 & \cdots \\ \vdots & \vdots & \ddots \end{bmatrix}. \tag{5}$$

The diagonal quantities, $q_i$, are the intensity of passage in units of $\mathrm{s}^{-1}$, given that the Markov process is in state $i$. The off-diagonal quantities, $q_{ij}$, are the intensity of transition to $j$, given that the Markov process is in state $i$ [15]. The transition intensities are commonly normalized such that

$$q_i = \sum_{j \neq i} q_{ij}, \tag{6}$$

but this is unnecessary for cases in which an absorbing state is left undefined.[1] For a purely absorbing state, $q_i = 0$. In the application to nuclide depletion, the entrants of the $\mathbf{Q}$ matrix are transition rates between nuclides, where $q_i$ is the removal rate of nuclide $i$, and $q_{ij}$ is the transition rate from nuclide $i$ to nuclide $j$. These transitions are governed by probabilities, decay constants, cross sections, and fluxes. With nuclides as the discrete state space, the $\mathbf{Q}$ matrix characterizes the isotopic changes in a given material due to irradiation and decay. Conveniently, this $\mathbf{Q}$ matrix is the transpose of the transition matrix $\mathbf{A}$. The entries of $\mathbf{A}^{\mathrm{T}}$ resemble the transition rates characterizing this continuous-time Markov chain.

[1] $\mathbf{A}^{\mathrm{T}}$ will never satisfy this condition due to fission (i.e., fission removes a single nuclide and adds several).

## II.A. DEFINITION OF REMOVED STATES

The formulation of the $\mathbf{A}^{\mathrm{T}}$ matrix given in Eq. (4) only includes nuclides that physically exist in a given material, and the formulation applies only to that material. Expanding the $\mathbf{Q}$ matrix to include $\mathbf{A}^{\mathrm{T}}$ and an additional state space that contains nuclides that no longer exist in the irradiated material enables the calculation of integral quantities (e.g., defining a state as nuclide i generated by fission) [16] and removed materials. The ability to calculate removed materials is imperative to MSR operations, as appropriately characterizing and tracking the waste streams from online salt separations and treatments is integral to these designs. Expanding the $\mathbf{Q}$ matrix to include removed nuclides increases the matrix size to $2M$,

$$\mathbf{Q} = \begin{bmatrix} & & \lambda_{1,\mathrm{rem}} & & \\ & \mathbf{A}^{\mathrm{T}} & & \ddots & \\ & & & & \lambda_{M,\mathrm{rem}} \\ \lambda_{1,\mathrm{rec}} & & -\lambda_1 - \lambda_{1,\mathrm{rec}} & & \\ & \ddots & & \ddots & \\ & & \lambda_{M,\mathrm{rec}} & & \end{bmatrix}, \tag{7}$$

provided all $M$ nuclides have a non-zero removal rate[2], and $\lambda_{i,\mathrm{rec}}$ is the recovery constant defining the continuous recovery of nuclide i from the waste stream back into the irradiated material.[3] This expansion adds over $3M$ non-zero elements to the $\mathbf{Q}$ matrix, as the assumption is the waste material is not undergoing irradiation, but includes radionuclide decay physics for the waste material. The nuclide vector $\boldsymbol{N}(t)$ has a length of $2M$, where the first $M$ elements describe the nuclide concentrations in the irradiated material, and the next $M$ elements describe the nuclide concentrations in the waste stream. Using matrix notation ($\mathbf{\Lambda}_{\mathrm{rem}}$, $\mathbf{\Lambda}_{\mathrm{rec}}$, and $\mathbf{B}$) for the removal and recovery diagonal submatrices and the decay/recovery submatrix of the $\mathbf{Q}$ matrix simplifies the matrix notation to

$$\mathbf{Q} = \begin{bmatrix} \mathbf{A}^{\mathrm{T}} & \mathbf{\Lambda}_{\mathrm{rem}} \\ \mathbf{\Lambda}^{\mathrm{rec}} & \mathbf{B} \end{bmatrix}. \tag{8}$$

This formulation may be expanded to include $W$ separate waste streams (e.g., to simulate removal and decay of $^{232}$Pa in batches for a thorium-based MSR):

$$\mathbf{Q} = \begin{bmatrix} \mathbf{A}^{\mathrm{T}} & \mathbf{\Lambda}_{1,\mathrm{rem}} & \cdots & \mathbf{\Lambda}_{W,\mathrm{rem}} \\ \mathbf{\Lambda}_{1,\mathrm{rec}} & \mathbf{B}_1 & & \\ \vdots & & \ddots & \\ \mathbf{\Lambda}_{W,\mathrm{rec}} & & & \mathbf{B}_W \end{bmatrix}. \tag{9}$$

[2] In most cases, only a few elements will have non-zero removal rates, so the matrix size will be much smaller than $2M$, and the submatrices will no longer be square diagonal.

[3] In most cases, there will be little or no elements fed back into the irradiated salt from the waste stream.

## II.B. DEFINITION OF MULTIPLE IRRADIATED STATES

Some MSR designs contain multiple zones and multiple fluids to maximize fuel utilization and overall core performance. In single-fluid multiple-zone designs, molten salts are mixed before and after they flow through the core. In multiple-fluid designs, the molten salts are always separate, and material is fed between the streams. For example, in a fast spectrum MSR, $^{239}$Pu bred in the blanket salt is fed to the driver salt. Expanding the **Q** matrix to include $Z$ irradiated materials requires the definition of additional diagonal matrices to define the nuclide transition rates from irradiated material $j$ to $k$,

$$\mathbf{\Lambda}_{jk} = \begin{bmatrix} \lambda_{1,jk} & & \\ & \ddots & \\ & & \lambda_{M,jk} \end{bmatrix}, \tag{10}$$

where $\lambda_{i,jk}$ is the transition constant defining the continuous feed of nuclide $i$ from the irradiated material $j$ to irradiated material $k$. Using this notation, the **Q** matrix is expanded to include the multiple irradiated zones:

$$\mathbf{Q} = \begin{bmatrix} \mathbf{A}_1^{\mathrm{T}} & \mathbf{\Lambda}_{12} & \cdots & \mathbf{\Lambda}_{1Z} \\ \mathbf{\Lambda}_{21} & \mathbf{A}_2^{\mathrm{T}} & \cdots & \mathbf{\Lambda}_{2Z} \\ \vdots & \vdots & \ddots & \vdots \\ \mathbf{\Lambda}_{Z1} & \mathbf{\Lambda}_{Z2} & \cdots & \mathbf{A}_Z^{\mathrm{T}} \end{bmatrix}. \tag{11}$$

This expansion adds a non-negligible number (approximately $60Z$ thousand) of non-zero matrix elements to **Q**. With the definition of waste streams, the generic form of **Q** is

$$\mathbf{Q} = \begin{bmatrix} \mathbf{A}_1^{\mathrm{T}} & \cdots & \mathbf{\Lambda}_{1Z} & \mathbf{\Lambda}_{11,\mathrm{rem}} & \cdots & \mathbf{\Lambda}_{1W,\mathrm{rem}} \\ \vdots & & \vdots & \vdots & & \vdots \\ \mathbf{\Lambda}_{Z1} & \cdots & \mathbf{A}_Z^{\mathrm{T}} & \mathbf{\Lambda}_{Z1,\mathrm{rem}} & \cdots & \mathbf{\Lambda}_{ZW,\mathrm{rem}} \\ \mathbf{\Lambda}_{11,\mathrm{rec}} & \cdots & \mathbf{\Lambda}_{1Z,\mathrm{rec}} & \mathbf{\Lambda}_1 & & \\ \vdots & & \vdots & & \ddots & \\ \mathbf{\Lambda}_{W1,\mathrm{rec}} & \cdots & \mathbf{\Lambda}_{WZ,\mathrm{rec}} & & & \mathbf{\Lambda}_W \end{bmatrix}. \tag{12}$$

This expansion of the **Q** matrix adds terms to the ODEs, as shown in Eq. (1), to account for removal and recovery mechanisms. For nuclide $i$ in irradiated material $k$, the ODE becomes

$$\begin{aligned} \frac{dN_i}{dt} = &\sum_{j\neq i}^{M} \left(l_{ij}\lambda_j + f_{ij}\sigma_j\phi\right) N_j(t) \\ &- \left(\lambda_i + \sum_j^W \lambda_{i,kj,\mathrm{rem}} + \sigma_i\phi\right) N_i(t) \\ &+ \sum_j^W \lambda_{i,jk,\mathrm{rec}} N_i^j(t) + \sum_j^Z \lambda_{i,jk} N_i^j(t) + S_i(t), \end{aligned} \tag{13}$$

where
$\lambda_{i,jk,\mathrm{rem}}$ is the removal constant defining continuous removal of nuclide $i$ from irradiated material $j$ to waste stream k,
$\lambda_{i,jk,\mathrm{rec}}$ is the recovery constant defining the continuous recovery of nuclide $i$ from waste stream $j$ back into irradiated material k, and
$N_i^j(t)$ is the concentration of nuclide $i$ in waste stream or irradiated material $j$.
For nuclides in waste material $k$, the ODEs become

$$\frac{dN_i}{dt} = \sum_j^Z \lambda_{i,jk,\mathrm{rem}} N_i^j(t) - \left(\lambda_i + \sum_j^Z \lambda_{i,kj,\mathrm{rec}}\right) N_i(t). \tag{14}$$

While a direct solution to a largely expanded **Q** matrix may be possible considering newly developed depletion solvers [16], in order to maintain the legacy behavior of ORIGEN and its philosophy to deplete only one material at a time, an alternative numerical approach is necessary. Still, it is a useful exercise to formulate this problem mathematically as the basis of an effective numerical solution scheme.

## II.C. NUMERICAL SOLUTION

It is possible to approximate systems with these complex feed, removal, and recovery mechanisms without directly changing the **Q** matrix. Implementation of these numerical solutions is simple for basic systems, such as a single irradiated material with continuous removals and no recovery. A generic numerical solution has several steps:

1. Assume that there are no materials in the waste streams for all times (i.e., $N_i^j(t) = 0$ for $j = 1, \ldots, W$ and for all nuclides $i$) in Eq. (13). Assume that there are no materials in the other irradiated material streams for all times (i.e., $N_i^j(t) = 0$ for $j = 1, \ldots, Z$ and for all nuclides $i$) in Eq. (13). These assumptions simplify the ODE such that is solvable by current methods (Eq. 1),

$$\begin{aligned} \frac{dN_i}{dt} = &\sum_{j\neq i}^{M} \left(l_{ij}\lambda_j + f_{ij}\sigma_j\phi\right) N_j(t) \\ &- \left(\lambda_i + \sum_j^W \lambda_{i,kj,\mathrm{rem}} + \sigma_i\phi\right) N_i(t) + S_i(t). \end{aligned} \tag{15}$$

2. Calculate the nuclide concentrations in irradiated materials $k = 1, \ldots, Z$.

3. Generate source terms from the nuclide concentrations in the irradiated materials $N_i^j(t)$ for $j = 1, \ldots, Z$ using the first term on the right hand side of Eq. (14):

$$S_i(t) = \sum_j^Z \lambda_{i,jk,\mathrm{rem}} N_i^j(t). \tag{16}$$

Treat this removal term as a source term.

4. Calculate the nuclide concentrations in waste streams $k = 1, \ldots, W$.

5. Generate source terms from the nuclide concentrations in the irradiated materials and waste streams,

$$S_i(t) = \sum_j^W \lambda_{i,jk,\mathrm{rec}} N_i^j(t) + \sum_j^Z \lambda_{i,jk} N_i^j(t) + S_i(t). \tag{17}$$

Treat these recovery and material flow terms as source terms.

6. Repeat steps 2–5 until the nuclide concentrations converge in the irradiated materials and waste streams.

For a single-material system with removals and no recovery, which is the most common case, only one pass through this algorithm is necessary.

## II.D. REMOVAL RATES

As shown in Eq. (4), the removal rates in this transition rate matrix formulation are defined as being similar to a decay constant in units of $s^{-1}$. This follows from the generic definition of design removal fraction,

$$N_i(t_{i+1}) = (1 - r_f)N_i(t_i), \tag{18}$$

where $t_i$ is the $i$th time step, $t_{i+1}$ is the following time step, and $r_f$ is the fraction of nuclide $i$ removed between time $t_i$ and $t_{i+1}$. Introducing the effective removal decay constant, $\lambda_r$, and treating the number densities as an exponential,

$$N_i(t) = N_i(0)e^{\lambda_r t} \tag{19}$$

yields a definition of this effective decay constant in terms of removal fraction and the efficiency of the removal process $\epsilon_r$,

$$\lambda_r = \frac{\ln\left|1 - r_f\epsilon_r\right|}{\Delta t}, \tag{20}$$

where $\Delta t$ represents the time required to remove $r_f$ of nuclide $i$ from the system, $r_f \in (0, 1]$, and $\epsilon_r \in (0, 1)$. This removal time depends on the efficiency of the removal equipment, the flow rate of the fuel, and the configuration defining the movement of the fuel to chemical processing equipment. ORNL MSR literature introduces the concept of cycle time to define the amount of time necessary to remove all of a given element from the fuel salt. Thus, for a removal process with a cycle time of 60 minutes and a 99.9% removal efficiency, the effective removal decay constant is

$$\lambda_r = \frac{\ln|1 - 1 \times 0.999|}{3600\text{s}}, \tag{21}$$

## III. IMPLEMENTATION AND TESTING

The SCALE implementation for these methods requires development in several tools within the code base. These tools include the point depletion solver ORIGEN, the neutron transport-depletion coupling interface in SCALE/TRITON, the 2D transport solver SCALE/NEWT, and a generic precursor drift solver. These implementations are tested for simple problems representative of potential applications [17] for these tools.

## III.A. POINT DEPLETION SOLVERS

ORIGEN already allows the addition of a removal rate for a given isotope to a given mixture's transition rate matrix, but (1) this capability is only accessible directly through the ORIGEN input, and (2) the current functionality is not designed to track and decay the material being removed. The new implementation addresses these issues, using removal and feed material classes to store information—isotopes and their removal/feed rates—and developing the means in ORIGEN to take this information, add the appropriate constants to a given material's transition rate matrix without expanding it, perform the depletion and decay steps, and optionally track the amount of materials being removed.

A common element of the iterative numerical solution (§ II.C.) is a removal term that must be recast as a feed term for mixtures that receive materials from other mixtures. This is achieved by specifying that the removed materials be tracked, pulling the removed material amounts, and generating a corresponding feed from these removed amounts. The removed material is tracked so that the amount removed at the end of a time step is consistent with that removed from a given mixture, as there may be some differences within a given time step. Any issues due to this approximation are expected to be second order effects.

An example for a two-mixture material flow (Fig. 1) is as follows:

1. Generate the removal class $r$ for mixture 1 using the list of desired isotopes and removal constants for each isotope.
2. Add the removal class $r$ to mixture 1.
3. Specify that the removal amounts be tracked for mixture 1.
4. Perform an ORIGEN solve for mixture 1 over the time step.
5. Get the amount removed from mixture 1 (i.e., isotopes and amounts).
6. Calculate the feed rate from the average removal rate from mixture 1.
7. Generate the feed class $f$ using the list of isotopes and average removal rates from mixture 1.
8. Add the feed class $f$ to mixture 2.
9. Perform an ORIGEN solve for mixture 2 over the time step.

This functionality is demonstrated and validated for two representative three-mixture problems with an irradiated mixture of $^{233}$U (5%) and $^{232}$Th (mixture 1) and initially empty waste mixtures (mixtures 2 and 3). Protactinium and neodymium are continuously removed from the irradiated mixture and fed into the waste mixtures (Fig. 2). This is a rough

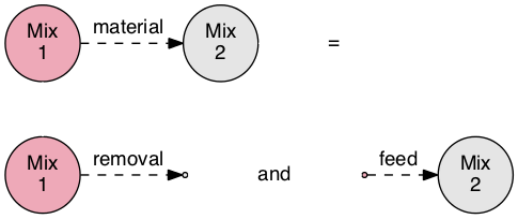


Fig. 1. Diagram of a two-mixture material flow example.

representation of some of the elemental removals in a thorium-fueled MSR system, where the beta decay product $^{233}$Pa from neutron capture in $^{232}$Th is removed to decay into fissile $^{233}$U before recycling back into the core. The important isotopes in this system are governed by the following set of equations:

$$\frac{dN_{\text{Pa-233,1}}}{dt} \approx -\lambda_{\text{Pa-233}} N_{\text{Pa-233,1}} - r_{\text{Pa,1}\to 2} N_{\text{Pa-233,1}} - r_{\text{Pa,1}\to 3} N_{\text{Pa-233,1}} + \lambda_{\text{Th-233}} N_{\text{Th-233,1}}, \quad (22)$$

$$\frac{dN_{\text{Pa-233},i}}{dt} \approx -\lambda_{\text{Pa-233}} N_{\text{Pa-233},i} + r_{\text{Pa,1}\to i} N_{\text{Pa-233,1}} \quad \text{for mixtures} \quad i = 2, 3, \quad (23)$$

$$\frac{dN_{\text{U-233},i}}{dt} \approx \lambda_{\text{Pa-233}} N_{\text{Pa-233},i} \quad \text{for mixtures} \quad i = 2, 3, \quad (24)$$

$$\frac{dN_{\text{Nd-148},i}}{dt} = r_{\text{Nd,1}\to i} N_{\text{Nd-148,1}} \quad \text{for mixtures} \quad i = 2, 3, \quad (25)$$

where $N_{X,i}$ is the number density of isotope $X$ in mixture $i$, $\lambda_X$ is the decay constant for isotope $X$, and $r_{X,i\to j}$ is the removal constant from mixture $i$ to mixture $j$ for element $X$ (Table I). The asymptotic behavior of this system of equations yields simple relations that are used to generate analytical solutions for $N_{\text{Pa-233},i}$ for $i = 1, 2, 3$, and $N_{\text{U-233},i}$ and $N_{\text{Nd-148},i}$ for $i = 2, 3$, using the $N_{\text{Th-233,1}}$ and $N_{\text{Nd-148,1}}$ concentrations from the ORIGEN calculation, as these are defined by the flux in mixture 1.

With the relatively high removal rates for protactinium, there is very little protactinium remaining in the irradiated mixture during operation (Fig. 3). After ~50 days, the concentration of $^{233}$Pa within each waste mixture reaches an equilibrium dictated by its constant generation (removal from mixture 1) and decay rates. The relative ratio of $^{233}$Pa in the two waste mixtures is dictated by the magnitude of the removal constants.

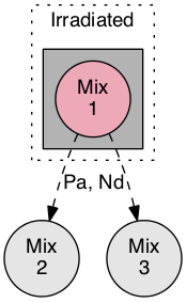


Fig. 2. Diagram of the material flows for this three-mixture problem 1 and 2.

TABLE I. Constants for the two ORIGEN test problems (units in inverse seconds).

| Parameter | Problem 1 | Problem 2 |
|---|---|---|
| $r_{\text{Pa,1}\to 2}$ | 0.1 | 0.3 |
| $r_{\text{Pa,1}\to 3}$ | 0.2 | 0.2 |
| $r_{\text{Nd,1}\to 2}$ | 10. | 50. |
| $r_{\text{Nd,1}\to 3}$ | 20. | 20. |
| $\lambda_{\text{Pa-233}}$ | $5.29201 \times 10^{-4}$ | |
| $\lambda_{\text{Th-233}}$ | $2.97495 \times 10^{-7}$ | |

For example, twice as much $^{233}$Pa is present in mixture 3 relative to mixture 2. The amount of $^{233}$U, the decay product of $^{233}$Pa (~27 day half-life), continuously increases, as it is not removed, and the waste material is not irradiated (Fig. 4). The rate of increase is constant and is proportional to the concentration of $^{233}$Pa in the given mixture. Similarly, the stable isotope $^{158}$Nd in the waste mixtures continuously increases at a constant rate; the relative ratio in the waste mixtures is again dictated by the removal rate (Fig. 5). In all cases, the numbers of each isotope reach their expected asymptotic value from manipulation of the Bateman equations. These observations verify that the ORIGEN tool is properly treating and quantifying the material removals for all three mixtures in the problem.

### III.B. TRANSPORT-DEPLETION COUPLING

The SCALE/TRITON module manages the coupling between neutron transport and point depletion modules within SCALE, passing pertinent information to each module within data containers. Thus, additional information to perform the continuous feed and removals (i.e., isotope list, constants, and mixture information) is added to these data containers, and ORIGEN is instructed to use this removal and feed information. For tracking removed isotopes, a target decay-only (i.e., unirradiated) mixture is defined within the SCALE/TRITON input, and the appropriate information is passed within these data containers. For more complex material flow systems (i.e., systems with material feedback loops), an iteration is required to generate an accurate solution. This iteration is designed to converge the feed rate of materials between the different mixtures for a problem in which they are interdependent. A large portion of this development work is accurately communicating mixture and flow information between TRITON and ORIGEN.

In the simulation, the notable difference between the SCALE/TRITON sequence and the standalone ORIGEN calculation is that the cross sections and fluxes used in the point depletion solve are generated from a neutron transport simulation (Fig. 2). Thus, a relation similar to that described in Eqs. (22)–(25) still holds, though an equivalent result to the ORIGEN simulation will not be obtained through the SCALE/TRITON input. For these implementation test problems, the same standalone ORIGEN problem material flow parameters are used (Table I). The asymptotic expected concentrations of $^{233}$Pa agree with the SCALE/TRITON-calculated concentrations after ~100 days (Fig. 6), which is similar to that seen in the standalone ORIGEN solution. The concentrations continue to increase in time as the material is irradiated because the fluxes and cross sections are updated at each neutron transport pass. Both the $^{233}$U and $^{148}$Nd concentrations in waste mixtures 2 and 3 increase at the expected asymptotic rate after a short period of time (Fig. 7 and 8). These implementation test problems ensure that the material flows between mixtures are functioning as expected when used through the SCALE/TRITON input.

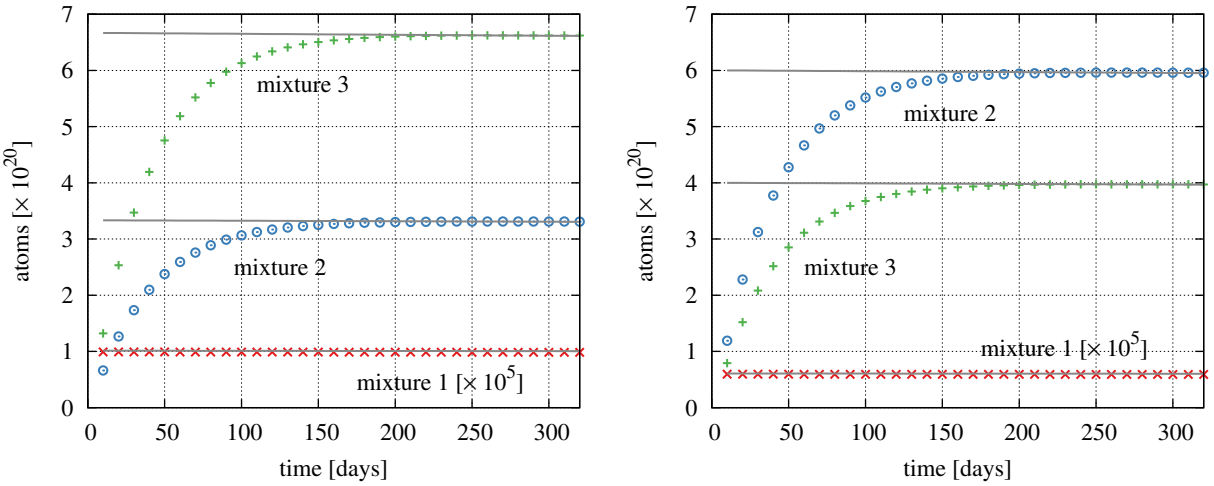


Fig. 3. Number of $^{233}$Pa atoms in problem 1 (left) and problem 2 (right) in each of the three mixtures.

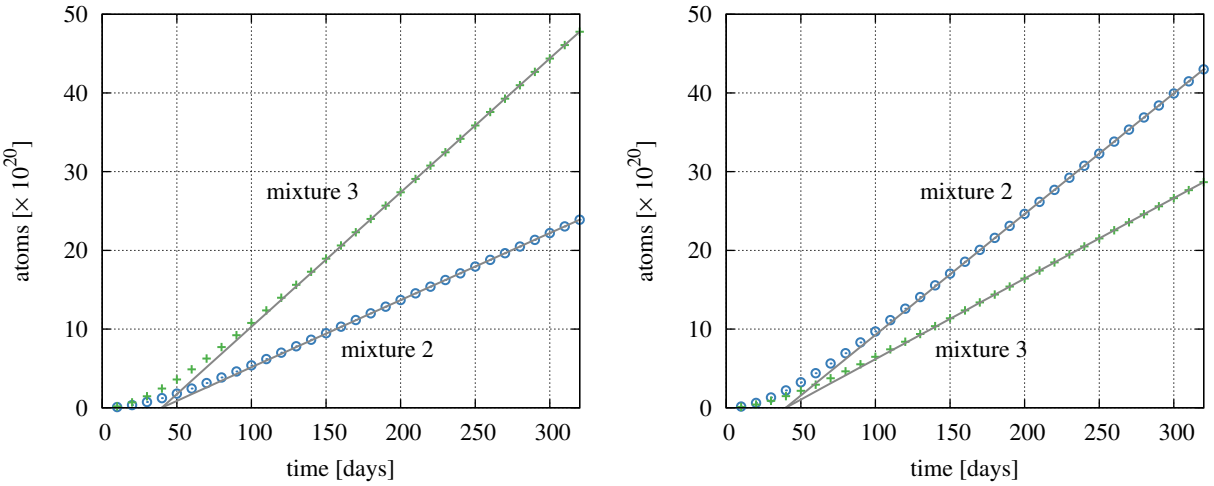


Fig. 4. Number of $^{233}$U atoms in problem 1 (left) and problem 2 (right) in the two waste mixtures.

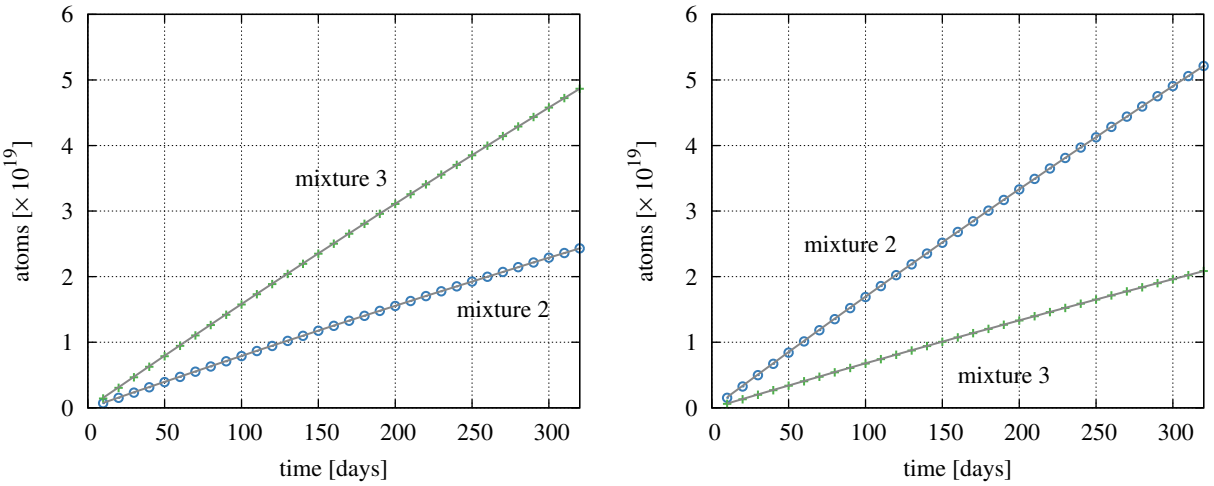


Fig. 5. Number of $^{148}$Nd atoms in problem 1 (left) and problem 2 (right) in the two waste mixtures.

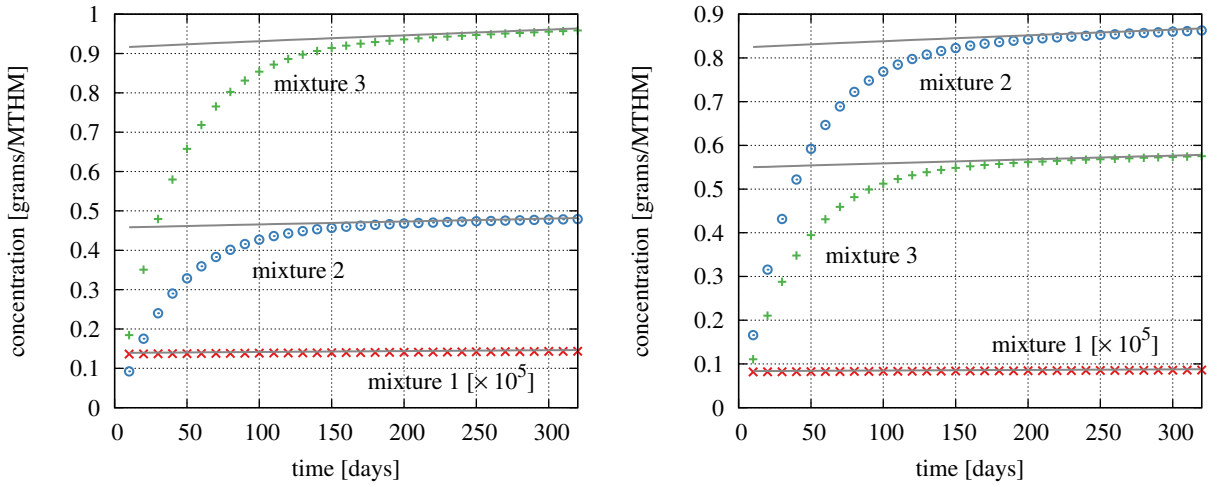


Fig. 6. Concentration of $^{233}$Pa in problem 1 (left) and problem 2 (right) in each of the three mixtures.

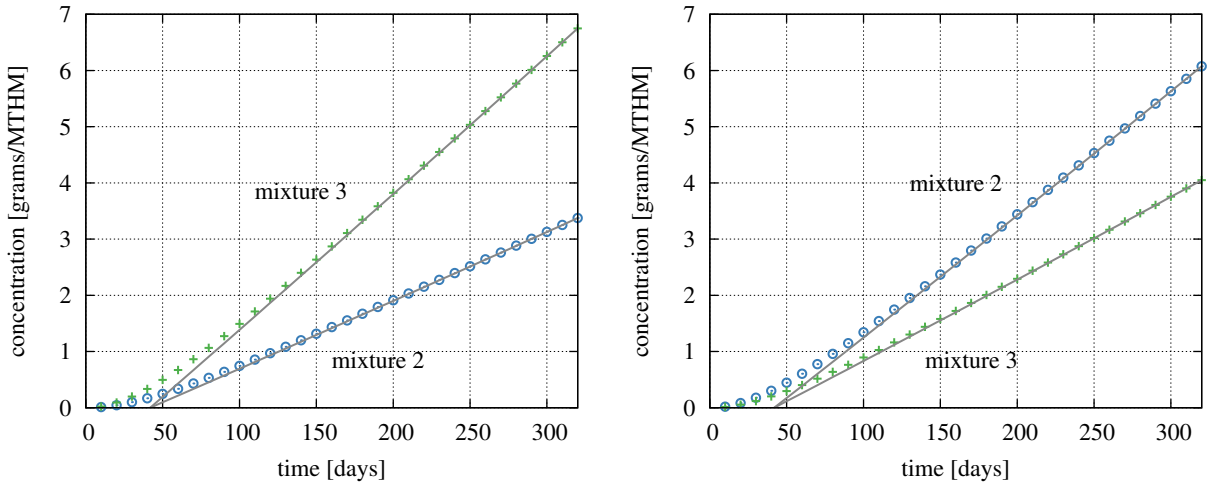


Fig. 7. Concentration of $^{233}$U in problem 1 (left) and problem 2 (right) in the two waste mixtures.

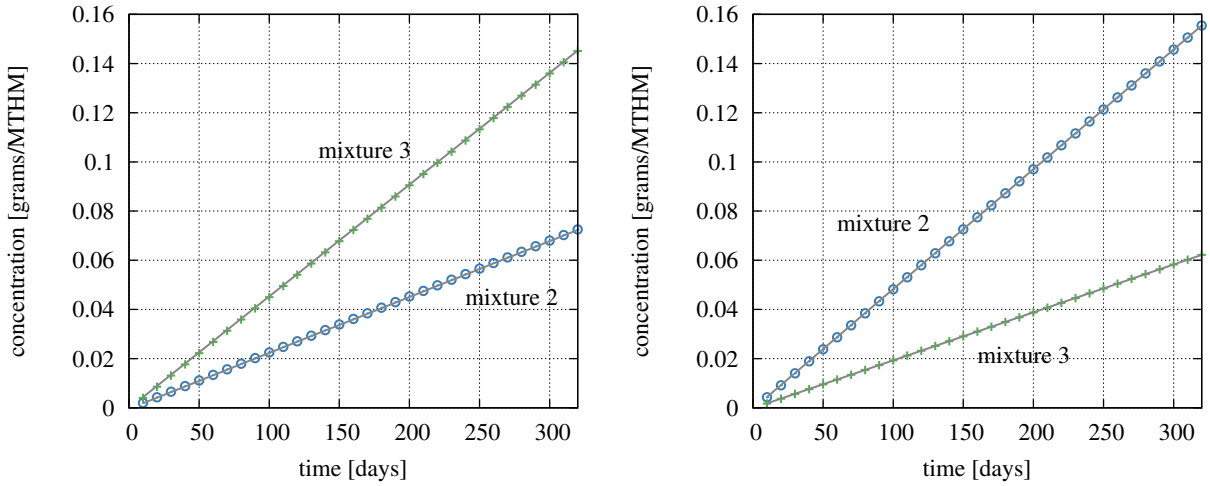


Fig. 8. Concentration of $^{148}$Nd in problem 1 (left) and problem 2 (right) in the two waste mixtures.

## IV. APPLICATION

A set of use cases (Table II) ordered with increasing complexity identifies the potential applications for this functionality. Each use case draws on documented MSR designs to encompass potential material processing definitions: the Molten Salt Reactor Experiment (MSRE), Molten Salt Breeder Reactor (MSBR), or Molten Chloride Fast Breeder Reactor (MCFBR). With protactinium recycling and rare earth element removals, the MSBR design is seen as a high-processing design that bounds many of the modern MSR developer concepts. Several variants of these cases were generated to ensure proper characterization of the system when using multiple feed, fuel, and waste mixtures. These variants are designed to effectively have the same geometries and material flow descriptions. For the results herein, all use cases use the same transport model, the same initial material compositions (Table III), and the same set of removal rate constants (Table IV).

Use case 0 serves as a control case in which the current capabilities of the SCALE/TRITON sequence are demonstrated (i.e., depletion without removals or additions to the fuel salt material). Use cases 1 and 4 (Fig. 9) tests removals only, use case 2 tests feeds only, and use cases 3 and 5 (Fig. 10) test both removals and feeds simultaneously. The previous ChemTriton semicontinuous batch method [10] for simulating these use cases serves as a tool for a code-to-code benchmark. Due to the use of a separate methodology and approach, the results from the SCALE/TRITON and ChemTriton tools are not expected to be identical.

All variants of each case are verified to ensure identical behavior in $k_\infty$ and isotopic compositions. In addition, the paired cases—1, 4, and 3, 5—are verified to ensure identical behavior in $k_\infty$ and isotopic composition of the fuel material. This ensures proper handling of the material removals and fuel

TABLE II. Summary of the use cases.

| Use Case | Feed | Removal | Tracked Waste | Waste Feedback | Variants |
|---|---|---|---|---|---|
| 0 | — | — | — | — | 2 |
| 1 | — | Yes | — | — | 3 |
| 2 | Yes | — | — | — | 3 |
| 3 | Yes | Yes | — | — | 3 |
| 4 | — | Yes | Yes | — | 5 |
| 5 | Yes | Yes | Yes | — | 6 |

TABLE III. Unit cell problem characteristics.

| Parameters | Value | |
|---|---|---|
| fuel temperature [K] | 909 | |
| graphite temperature [K] | 900 | |
| graphite density [g/cc] | 1.843 | |
| fuel channel radius [cm] | 2.59917 | |
| fuel channel pitch [cm] | 10.16 | |
| cross section library | 56-group ENDF/B-VII.1 [18] | |
| fuel isotopic composition [g/cc] | $^{19}$F | 1.48999 |
| | $^{233}$U | 0.02397 |
| | $^{232}$Th | 1.43197 |
| | $^{7}$Li | 0.25870 |
| | $^{9}$Be | 0.07416 |

TABLE IV. Removal constants for the use cases.

| Processing group | Elements | Constant ($s^{-1}$) |
|---|---|---|
| Volatile gases | Xe, Kr | $3.4539\times10^{-1}$ |
| Noble metals | Se, Nb, Mo, Tc, Ru, Rh, Pd, Ag, Sb, Te | $3.4539\times10^{-1}$ |
| Seminoble metals | Zr, Cd, In, Sn | $3.9975\times10^{-7}$ |
| Volatile fluorides | Br, I | $1.3325\times10^{-6}$ |
| Rare earth elements | Y, La, Ce, Pr, Nd, Pm, Sm, Gd | $1.5990\times10^{-6}$ |
| | Eu | $1.5990\times10^{-7}$ |
| Discard | Rb, Sr, Cs, Ba | $2.3275\times10^{-8}$ |

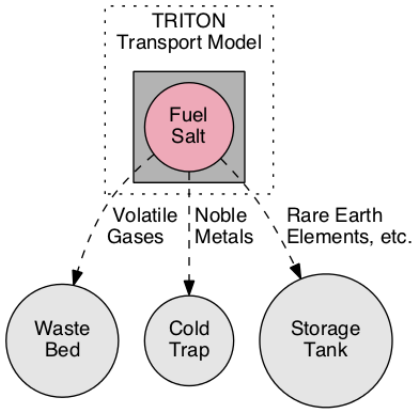


Fig. 9. Use cases 1 and 4 have material removals to external mixtures, which may (case 1) or may not (case 4) be decayed and tracked along with the fuel salt mixture (MSBR without fueling or protactinium recycle).

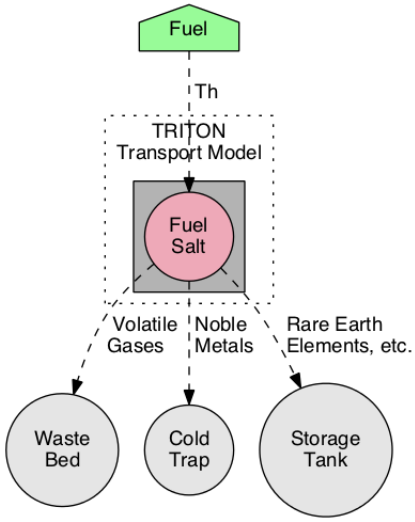


Fig. 10. Use cases 3 and 5 have a fuel feed from an external source and material removals to external mixtures, which may (case 3) or may not (case 5) be decayed and tracked along with the fuel salt mixture (MSBR without protactinium recycle).

additions when operating with $n$ number of feeds, removals, and fuel materials. Results are comprehensive, but they are not shown.

Next, results (e.g., $k_\infty$, isotopic compositions) from the use cases are reviewed for expected behavior. Without removals, fission product poisons continuously build up within the fuel salt, and the unit cell $k_\infty$ decreases during operation (Fig. 11). Thus, use cases 0 and 2 have the lowest $k_\infty$ over the first year, with use case 2 being the lowest due to the continuous feed of absorbing fertile material. With removals, the most absorptive fission products are continuously removed from the system, and the $k_\infty$ remains above 1.0. The small $\Delta k$ between use cases 0 and 2 is mirrored in use cases 1 and 3, where the fertile material feed decreases criticality.

Without a continuous feed of fertile material, the fuel salt thorium concentration decreases linearly, as it is converted to $^{233}$U (Fig. 12). Use cases 0 and 1 agree relatively well, though small differences in this concentration may have a large impact on $^{233}$U, as there is much more $^{232}$Th within the system. In use cases 2 and 3, the set feed rate is not sufficient to counteract the transmutation of $^{232}$Th, although the decrease in its concentration is very slow.

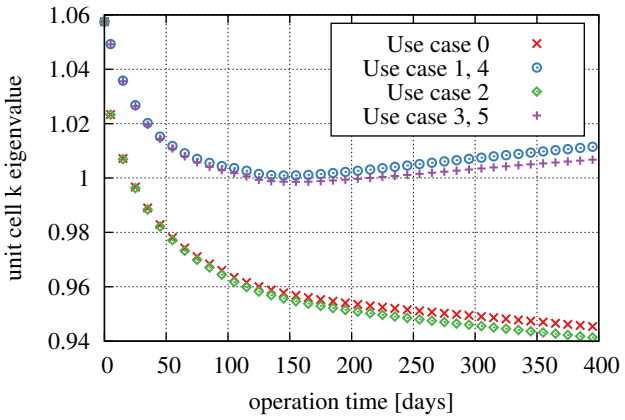


Fig. 11. Comparison of the $k_\infty$ of the first five use case problems.

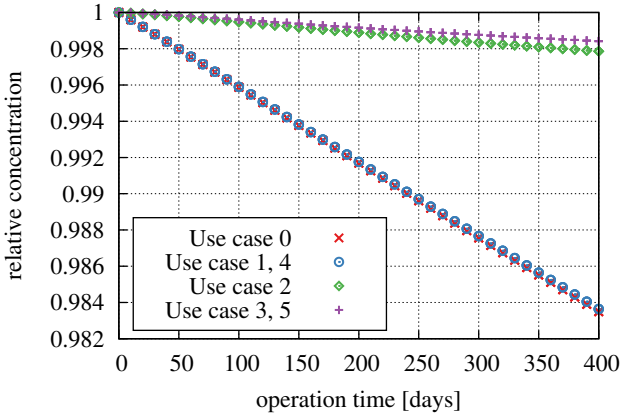


Fig. 12. Comparison of the $^{232}$Th concentrations in the fuel salt of the first five use case problems.

In all use cases, the concentration of $^{233}$U initially decreases before recovering as the $^{232}$Th transmutation reaches a steady rate (Fig. 13). For use cases 0 and 2, the $^{233}$U concentration recovers more quickly due to the harder spectrum induced by the presence (i.e., no removal) of fission product absorbers. The $^{233}$U recovers the quickest in use case 2, as the feed rate maintains a higher concentration of fertile $^{232}$Th within the fuel salt.

In use cases 0 and 2, the $^{148}$Nd concentrations within the fuel salt are nearly identical, increasing linearly in time (Fig. 14). This is expected, as the fission product isotope $^{148}$Nd is known to be a burnup marker; the generation rate of this isotope should be relatively constant during irradiation over lower burnups in this system. In use cases 1 and 3, neodymium is removed at a constant, continuous rate, causing the $^{148}$Nd concentration within the fuel salt to reach an asymptotic value. The concentrations in these two use cases is identical because both the generation and removal rates are the same.

Using equivalent unit cell models and three-day time steps in the ChemTriton simulations, comparable results for use

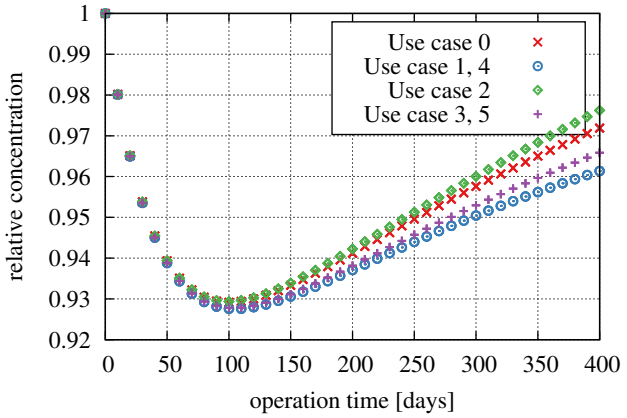


Fig. 13. Comparison of the $^{233}$U concentrations in the fuel salt of the first five use case problems.

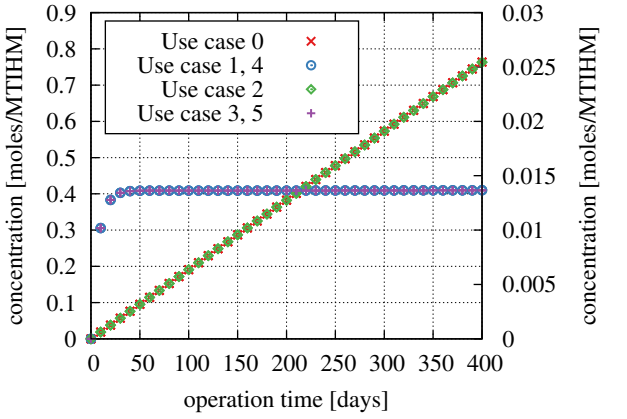


Fig. 14. Comparison of the $^{148}$Nd concentrations in the fuel salt of the first five use case problems. Use cases 1, 4 and 3, 5 use the secondary (right) axis.

cases 1, 2, and 3 were generated. Due to smaller time stepping, reporting of the initial time step $k_\infty$ for the ChemTriton results, and middlestep depletion methodology (which is performed without knowledge of the removals process), these simulations are not expected to yield results that are identical to the SCALE/TRITON simulations. For use case 1, the $k_\infty$ of the SCALE/TRITON trends similarly to the ChemTriton $k_\infty$, but it contains a few larger jumps at specific time points due to the middlestep method (Fig. 15). In use case 3, the agreement is very similar to the use case 1 trends (Fig. 16).

The transmutation of the fertile material in the ChemTriton and SCALE/TRITON simulations agree very well (Figs. 17–18), but different fertile feed conditions cause some differences between use cases 2 and 3. Due to the smaller amount of $^{233}$U within the fuel salt, it is more greatly impacted by smaller changes in transmutation rates. With the middlestep method, the ChemTriton simulation depletes with a flux that is calculated as if there were more fission products in the fuel salt than there actually should be. Thus, the spectrum is hardened, and more $^{232}$Th is transmuted. In addition, there is a small effect from the slightly higher concentration of fertile material within the ChemTriton simulation, slightly increasing

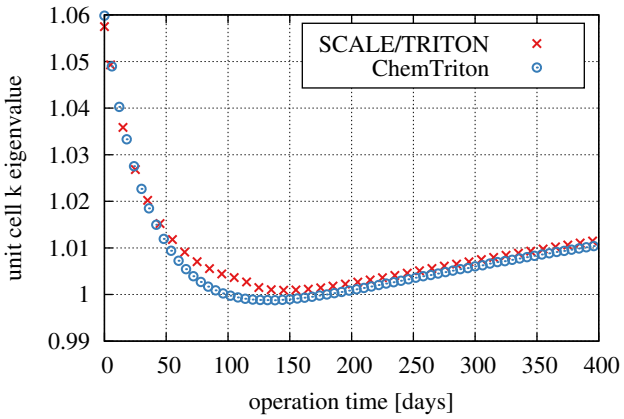


Fig. 15. Comparison of the $k_\infty$ between ChemTriton and SCALE/TRITON for use case 1.

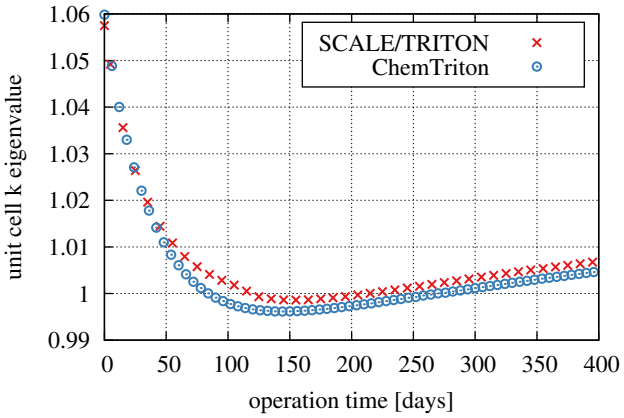


Fig. 16. Comparison of the $k_\infty$ between ChemTriton and SCALE/TRITON for use case 3.

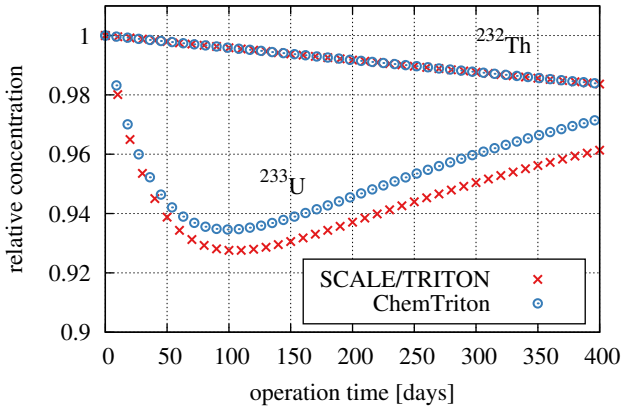


Fig. 17. Comparison of the fissile and fertile isotope concentrations between ChemTriton and SCALE/TRITON for use case 1.

the generation rate of $^{233}$U.

The ability to track and decay waste materials accurately is an additional functionality of major importance when determining storage needs and characterizing source terms. The ChemTriton tool has some limitations in this respect, specifically for nuclides with shorter half lives and large neutron absorption cross sections. For example, $^{135}$Xe reaches an equilibrium concentration within a reactor, which is dependent on the $^{135}$Xe fission yield, the decay of other nuclides (e.g., $^{135}$I), and the decay of $^{135}$Xe. Within these use cases, SCALE/TRITON adds a dependency to this problem: the defined removal rate of $^{135}$Xe. Thus, a lower (i.e., with respect to a case without removals) equilibrium concentration of $^{135}$Xe is reached within the fuel salt (Fig. 19). In use cases 1, 3, 4, and 5, the removal rate of xenon is very high, dominating most terms in this equation, resulting in a very low concentration of xenon within the fuel salt material. Because the method employed in ChemTriton uses a semicontinuous batch approach, the $^{135}$Xe is allowed to reach equilibrium over the course of a few days, after which all xenon is removed from the fuel

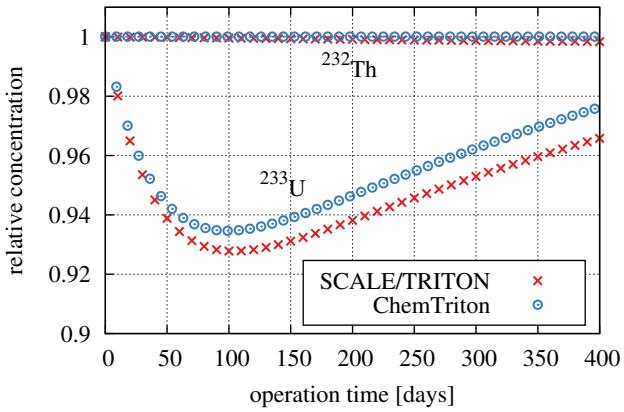


Fig. 18. Comparison of the fissile and fertile isotope concentrations between ChemTriton and SCALE/TRITON for use case 3.

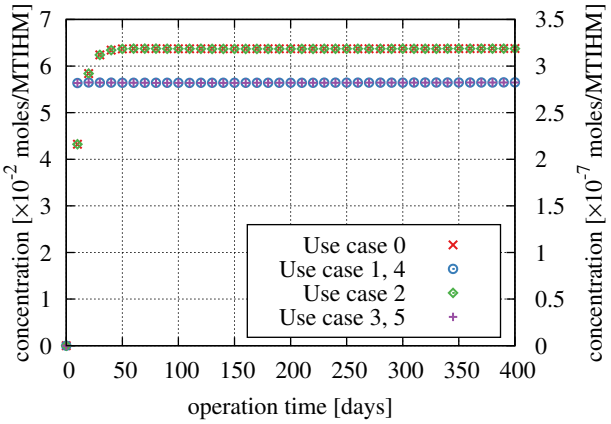


Fig. 19. Comparison of the $^{135}$Xe concentrations in the fuel salt of the first five use case problems. Use cases 1, 4 and 3, 5 use the secondary (right) axis.

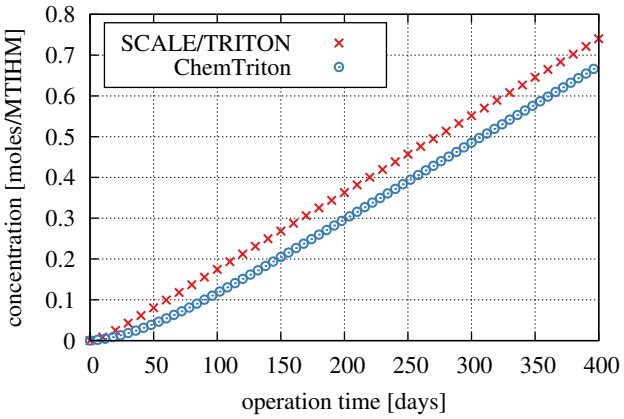


Fig. 20. Comparison of the total $^{148}$Nd concentrations within waste materials between SCALE/TRITON and ChemTriton simulations for use case 4.

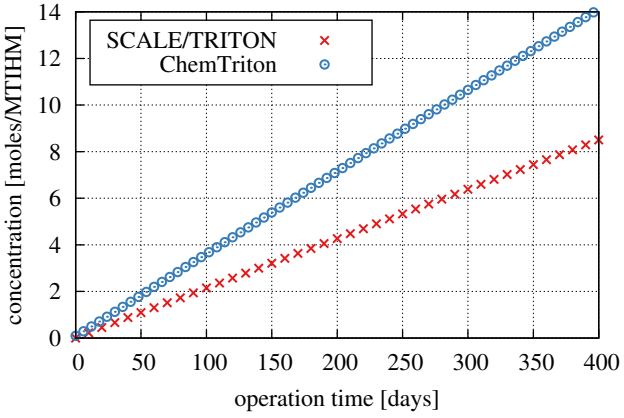


Fig. 21. Comparison of the total Xe concentrations within waste materials between SCALE/TRITON and ChemTriton simulations for use case 4.

salt. Then, this mass removal is averaged over the few-day step size into a removal rate; this rate is expected to be too low and nonconservative. The total amount of material within a waste mixture is understood from this rate.

These limitations cause large differences in the total amount of removed material masses for specific nuclides (Fig. 21). In addition, the radioactive (Fig. 22) and stable (Fig. 23) nuclides in an unirradiated waste mixture trend differently with time, with radioactive nuclides reaching an equilibrium concentration before decaying into different nuclides and/or elements. Thus, the isotopic and elemental composition of this removed waste material is continuously changing during reactor operation and after shutdown; this change must be accounted for when defining system waste form storage and disposal.

## V. CONCLUSIONS

A continuous removal and tracking capability has been implemented in the SCALE/TRITON module. The implementation has been tested using some comparisons to analytic solutions for simplified multiple mixture problems. Applications

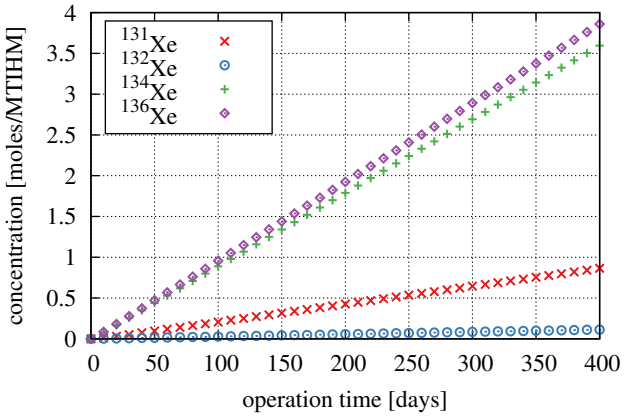


Fig. 22. Stable xenon isotopes in removed waste material for use case 4.

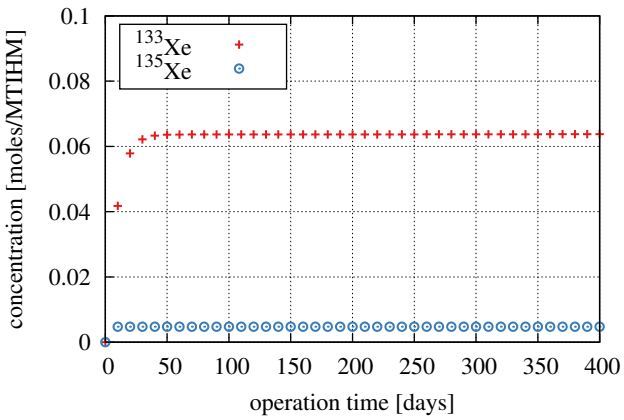


Fig. 23. Radioactive xenon isotopes in removed waste material for use case 4.

to six use case problems provide additional comparisons for relevant scenarios and comparisons to ChemTriton simulations. The SCALE-integrated tools compare well with ChemTriton simulations considering the differences and approximations inherent to the ChemTriton methodology. Additional capabilities were demonstrated in tracking waste stream materials that are important for molten salt reactor source term, safeguards, and component performance modeling.

## VI. ACKNOWLEDGMENTS

This work is supported by the US Department on Energy, Office of Technology Transitions, Technology Commercialization Fund.

## REFERENCES

1. S. BRINTON, "The Advanced Nuclear Industry," http://www.thirdway.org/report/the-advanced-nuclear-industry, Third Way (June 2015), Accessed March 1, 2016.
2. H. F. BAUMAN, G. W. CUNNINGHAM III, ET AL., "ROD: A Nuclear and Fuel-Cycle Analysis Code for Circulating-Fuel Reactors," Tech. Rep. ORNL-TM-3359, Oak Ridge National Laboratory (1971).
3. D. HEUER, E. MERLE-LUCOTTE, ET AL., "Towards the Thorium Fuel Cycle with Molten Salt Reactors," *Annals of Nuclear Energy*, **64**, 421–429 (2014).
4. C. FIORINA, M. AUFIERO, ET AL., "Investigation of the MSFR core physics and fuel cycle characteristics," *Progress in Nuclear Energy*, **68**, 153–168 (2013).
5. R. J. SHEU, C. H. CHANG, ET AL., "Depletion Analysis on Long-Term Operation of the Conceptual Molten Salt Actinide Recycler & Transmuter (MOSART) by Using a Special Sequence Based on SCALE6/TRITON," *Annals of Nuclear Energy*, **53**, 1–8 (2013).
6. M. AUFIERO, A. CAMMI, ET AL., "An Extended Version of the SERPENT-2 Code to Investigate Fuel Burn-Up and Core Material Evolution of the Molten Salt Fast Reactor," *Journal of Nuclear Materials*, **441**, 473–486 (2013).
7. A. AHMAD, E. B. MCCLAMROCK, and A. GLASER, "Neutronics Calculations for Denatured Molten Salt Reactors: Assessing Resource Requirements and Proliferation-Risk Attributes," *Annals of Nuclear Energy*, **75**, 261–267 (2015).
8. J. PARK, Y. JEONG, ET AL., "Whole Core Analysis of Molten Salt Breeder Reactor with Online Fuel Reprocessing," *International Journal of Energy Research*, **39**, 1673–1680 (2015).
9. J. J. POWERS, T. J. HARRISON, and J. C. GEHIN, "A New Approach for Modeling and Analysis of Molten Salt Reactors Using SCALE," in "Proc. Int. Conf. Mathematics and Computational Methods Applied to Nuclear Science and Engineering (M&C 2013)," Sun Valley, Idaho (2013).
10. B. R. BETZLER, J. J. POWERS, and A. WORRALL, "Molten Salt Reactor Neutronics and Fuel Cycle Modeling and Simulation with SCALE," *Annals of Nuclear Energy*, **101**, 489–503 (2017).
11. B. R. BETZLER, J. J. POWERS, N. R. BROWN, and B. T. REARDEN, "Molten Salt Reactor Neutronics Tools in SCALE," in "Proc. Int. Conf. on Mathematics and Computational Methods Applied to Nuclear Science and Engineering (M&C 2017)," Jeju, Korea (2017).
12. S. M. BOWMAN, "SCALE 6: Comprehensive Nuclear Safety Analysis Code System," *Nuclear Technology*, **174** (2011).
13. I. C. GAULD, G. RADULESCU, ET AL., "Isotopic Depletion and Decay Methods and Analysis Capabilities in SCALE," *Nuclear Technology*, **174**, 267–283 (2011).
14. G. G. DAVIDSON, T. M. PANDYA, ET AL., "Nuclide Depletion Capabilities in the Shift Monte Carlo Code," in "Proc. Int. Conf. PHYSOR 2016," Sun Valley, Idaho (2016).
15. S. M. ROSS, *Stochastic Processes*, John Wiley & Sons, Inc., New York (1996).
16. A. ISOTALO, "Calculating Time-Integral Quantities in Depletion Calculations," *Nuclear Science and Engineering*, **183**, 421–429 (2016).
17. A. RYKHLEVSKII, B. R. BETZLER, A. WORRALL, and K. D. HUFF, "Fuel Cycle Performance of Fast Spectrum Molten Salt Reactor Designs," in "Proc. Int. Conf. on Mathematics and Computational Methods Applied to Nuclear Science and Engineering (M&C 2019)," Portland, OR (2019).
18. M. B. CHADWICK, P. OBLOZINKY, ET AL., "ENDF/B-VII.1: Nuclear Data For Science and Technology: Cross Sections, Covariance, Fission Product Yields and Decay Data," *Nuclear Data Sheets*, **112**, 2887–2996 (2011).